trum may be once forbidden ($\Delta j=0, \pm 1$, yes!) or l-forbidden ($\Delta j=1$, no!, $\Delta l=2$). According to the former classification, the excited level at 0.73 ± 0.02 Mev in the residual nucleus Nb^{95}, could have the orbital $p_{3/2}$, $f_{5/2}$, or $f_{7/2}$. Were it either of the first two values, a relatively intense gamma-ray of energy ~ 0.5 Mev would be expected to appear among the radiations of Zr^{95}, emitted in the transition between the level at 0.73 ± 0.02 Mev and the 0.21-Mev metastable level of the 90-hr Nb^{95} (see Fig. 4). Only in the case of $f_{7/2}\rightarrow g_{9/2}$ does the probability of a transition to the ground state of Nb^{95} exceed that of a transition to the metastable level ($f_{7/2}\rightarrow p_{1/2}$). Since no gamma-radiation at 0.5 Mev is observed, the most likely of the three orbitals associated with the assumption of a once forbidden transition is $f_{7/2}$.

If an l forbidden beta-transition is assumed, the orbital assignment of the 0.73 ± 0.02 Mev level is uniquely $g_{7/2}$. The transition $g_{7/2}\rightarrow g_{9/2}$ is, of course, far more probable than $g_{7/2}\rightarrow p_{1/2}$. Since the $f_{7/2}$ shell closes at 28 nucleons, the $g_{7/2}$ subshell, closing at 58 nucleons, is favored.

From shell model considerations and the conversion coefficients of the 0.76 ± 0.02 Mev gamma-ray of Nb^{95}, it has been previously shown[15] that the decay of Nb^{95} to Mo^{95} can be characterized by $g_{9/2}\rightarrow g_{7/2}\rightarrow d_{5/2}$.

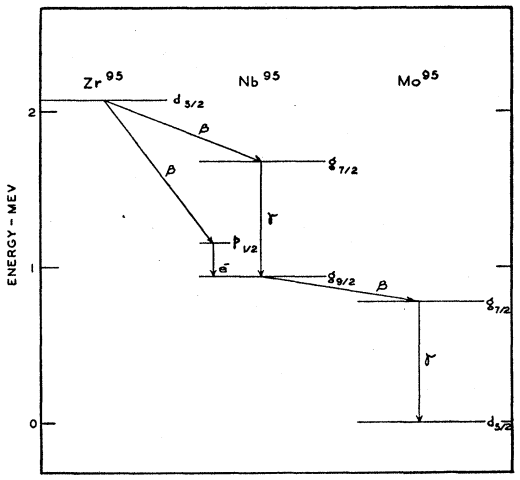

FIG. 4. Disintegration scheme of Zr^{95}—Nb^{95}.

[15] C. Y. Fan, Phys. Rev. **87**, 252 (1952).

PHYSICAL REVIEW VOLUME 89, NUMBER 3 FEBRUARY 1, 1953

Neutron Scattering by Coupled Paramagnetic Ions

PHILIP J. BENDT*
Pupin Physics Laboratories, Columbia University, New York, New York
(Received August 8, 1952)

The paramagnetic scattering of very low energy neutrons by MnF_2 and MnO was studied at various sample temperatures. The assumption of Van Vleck that a Gaussian distribution can be used to represent the frequency of inelastic scattering events *versus* energy transfer with the spin lattice is used, and the root mean square half-width of the distribution of energy transfer for MnF_2 is found to be 0.0020, 0.0026, and 0.0034 ev at 610°, 300°, and 126°K, respectively. Short-range order scattering modifies the scattering cross section for MnF_2 to the extent of $1.5/4\pi$ barns/steradian at 126°K, but is not observed at higher temperatures.

Measurements at 300°K indicate the magnetic scattering cross section for MnO, it if were not distorted by short-range order scattering, would be about $2.5/4\pi$ barns/steradian lower than for MnF_2. We suggest this may be accounted for by the mechanism of super-exchange between crystal ions. Rough values of a parameter indicating the range of spin order in MnO were determined at 300° and 133°K. The amount of spin order increases with decrease in sample temperature. Above the Néel temperature, it is found that most of the correlation of spin direction exists only between adjacent ions on the same sublattice.

INTRODUCTION

THE scattering of slow neutrons by crystal lattices of free paramagnetic ions has been examined experimentally.[1,2] For uncoupled ions, the magnetic scattering from each ion is incoherent relative to the nuclear scattering and the magnetic scattering from other ions. The principal feature observed is a magnetic form factor arising from the space distribution of paramagnetic electrons in the ion.

The scattering from antiferromagnetic[2] and ferromagnetic[3] materials has also been examined. For these materials, the spin state of the scatterer is assumed not to change in the scattering process, so the magnetic scattering is coherent and shows strong Bragg reflections.

Paramagnetic substances generally have a transition temperature below which there is long-range order of spin directions in the crystal lattice. This temperature T_0 is called the Curie temperature for those materials which become ferromagnetic, and the Néel temperature

* Now at the Los Alamos Scientific Laboratory, Los Alamos, New Mexico.

[1] I. W. Ruderman, Phys. Rev. **76**, 1572 (1949).

[2] Shull, Strauser, and Wollan, Phys. Rev. **83**, 333 (1951).

[3] C. G. Shull, Phys. Rev. **81**, 626 (1951).

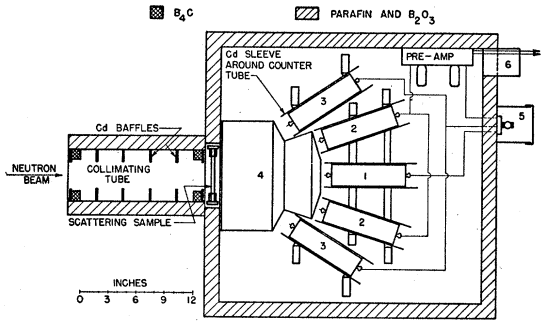

FIG. 1. Apparatus for detecting neutrons scattered at 18° and 33°.

for those materials which become antiferromagnetic. Above T_0 there is a temperature range in which the spins of neighboring paramagnetic ions are coupled.

This temperature range above T_0, where the ion spins are neither completely free nor completely locked in given directions, has not been investigated extensively. As a result of the coupling between the magnetic ions, the neutron scattering is spin-inelastic, involving energy transfer with the spin lattice. Van Vleck[4] has explained how this reduces, by two different processes, the amount of magnetic scattering which would be observed from free ions. Residual coherent scattering, derived from short-range order of spin directions among neighboring ions in a crystal lattice, contributes broad liquid-scattering type reflection patterns.

In the present experiment, measurements were made in the intermediate region above the Néel temperature of two antiferromagnetic compounds. Short-range order scattering and energy transfer between neutron and spin lattice were studied at several sample temperatures.

I. APPARATUS

The experiment was performed with a collimated beam of slow neutrons from the Columbia University cyclotron. The arc source of the cyclotron was pulsed, in order that the time-of-flight of the neutrons could be measured with the electronic Neutron Velocity Selector.[5]

The apparatus shown in Fig. 1 was built to detect the neutrons. A single BF_3 counter tube (1) is located in line with the incident neutron beam, and detects neutrons transmitted through the sample. Eight counter tubes (2) are mounted in a ring along elements of a cone having a mean half-angle of 18°. Twelve counter tubes (3) are mounted in a ring along elements of a similar cone with a half-angle of 33°. The apparatus was built to observe scattering at angles near the forward direction in order to avoid the coherent nuclear Debye-Scherrer rings.

Neutrons in the wavelength region in which measurements were made, 1.6 to 5.5 angstroms, are of sufficiently low energy that a 0.022-inch layer of cadmium provides efficient shielding. The neutron beam is defined with cadmium baffles, and the counter tubes are wrapped with cadmium, allowing neutrons to enter only through the ends. Shielding against stray neutrons is provided in the walls of the box containing the counter tubes. The collimating tube and aluminum container (4) were filled with argon gas to reduce air scattering in the vicinity of the sample. A "temperature cell" was constructed to hold samples at temperatures above or below room temperature while scattering measurements were being made. The sample temperature was measured with thermocouples.

The powder samples of anhydrous crystals of MnF_2 and MnO used in the experiment were prepared by Dr. I. W. Ruderman, and their preparation and handling are described in reference 1.

II. CALIBRATION OF THE APPARATUS

The scattering apparatus does not measure absolute cross sections, but must be calibrated with a standard scattering sample. The number of materials suitable for standards is very limited, owing to crystal structure interference effects, which strongly influence the scattering in the thermal energy region. An ideal material for a standard would be a heavy element with large incoherent scattering and negligible coherent scattering. An element which approximates the ideal standard is vanadium, which has a bound scattering cross section of 5.1 barns, a coherent scattering cross section of 0.1 barn, and a mass number of 51. Two samples of pure vanadium of different thickness were used to calibrate the scattering apparatus. A correction for multiple scattering was made by extrapolating to "zero thickness" where the ratio of multiple to single scattering goes to zero. The incoherent scattering from hydrogen in very thin sheets of polythene $(CH_2)_n$ was used to check the calibration.

The problem of separating the paramagnetic scattering from the nuclear scattering and multiple scattering

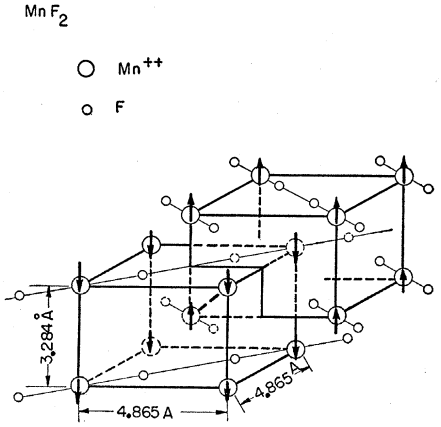

FIG. 2. The MnF_2 body-centered tetragonal lattice structure. Below T_0, the Mn^{++} ion spins are directed oppositely on the two interpenetrating sublattices.

[4] J. H. Van Vleck, Phys. Rev. **55**, 924 (1939).
[5] L. J. Rainwater and W. W. Havens, Jr., Phys. Rev. **70**, 136 (1946); **71**, 65 (1947).

must be considered. The isotope and spin nuclear incoherent scattering of Mn, F, and O are all essentially zero. The nuclear coherent scattering occurs at angles larger than 33° in the wavelength region in which paramagnetic scattering was studied. However, the nuclear coherent scattering can contribute through multiple scattering. The strongest nuclear Debye-Scherrer ring is oriented at 90° in MnF_2 at the wavelength 3.8 angstroms and at 90° in MnO at the wavelength 3.6 angstroms. As the coherently scattered neutrons near these wavelengths are traveling approximately in the plane of the sample, they have a very long path length in the sample and have a good chance of being scattered a second time. This means experimental data close to the above wavelengths have received a contribution from second-scattered neutrons. In determining the best smooth curve to fit the experimental data, the multiple scattering contribution to these points was corrected for, and therefore these points lie above the experimental curves.

At wavelengths other than those referred to above, the multiple scattering in MnF_2 and MnO is small, for two reasons. First, the samples are thin; the transmission calculated on the basis of the scattering cross section alone is about 0.9. Second, the capture cross section for Mn is large (13 barns at 1.8 angstroms), and this substantially reduces the ratio of multiple to single scattering. It is estimated that the contribution of nuclear incoherent scattering and multiple scattering is about $1/4\pi$ barns/steradian.

III. CRYSTAL STRUCTURE

MnF_2 has the body-centered tetragonal lattice shown in Fig. 2. The Mn ions are located on two inter-penetrating sublattices. In Fig. 2, the Mn spins are shown directed along the short edge of the unit crystal cell, parallel on each sublattice, and with spins opposite on the two sublattices. This is the antiferromagnetic arrangement of spins which exists in MnF_2 at temperatures below the Néel temperature 72°K as proposed by Erickson and Shull.[6]

The crystal structure of MnO resembles that of NaCl, and presents a face-centered cubic lattice of Mn ions. This can be separated into four inter-penetrating cubic sublattices of Mn ions, as shown in the top diagram of Fig. 3. Below the Néel temperature 122°K the spins are aligned alternately antiparallel on each sublattice, taken separately.[3] Consequently, each sublattice can be separated into two lattices of (+) and (−) spins, respectively, which are again f.c.c. but with a repeating distance of twice the length of the edge of a unit crystal cell. Magnetic Bragg reflections are indexed by Shull on the basis of these lattices of double size dimensions. The ion spins in Fig. 3 are directed along a crystal axis. They are parallel on alternate (1,1,1) planes and opposite on the intervening planes. This is the arrangement found by Shull, Strauser, and Wollan.[2]

[6] R. A. Erickson and C. G. Shull, Phys. Rev. **83**, 208 (1951).

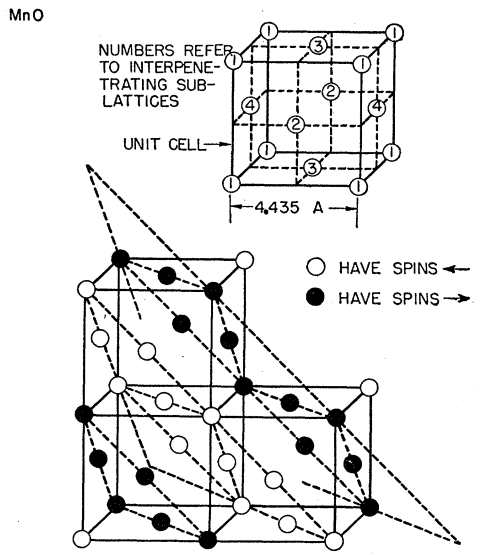

FIG. 3. The MnO face-centered cubic lattice structure. The lattice is similar to NaCl; oxygen atoms are not shown. Below T_0, Mn spins are opposite on alternate (1,1,1) planes.

Oxygen ions, not shown in Fig. 3, occur at the intersections of dashed lines with solid lines in the upper diagram, and in the center of the unit cell. Thus, each pair of adjacent Mn ions on one sublattice is separated by an oxygen ion, and ordinary quantum mechanical exchange cannot account for the antiparallel alignment of spins on the individual sublattices. The mechanism believed responsible for the spin arrangement was originated by Kramers and developed by Anderson[7] and Smart[8] for the case of f.c.c. compounds, and is called super-exchange. This involves assigning a weight in the total wave function to configurations in which a $2p$ electron from oxygen has transferred to a neighboring Mn ion. The other $2p$ electron on oxygen which has the same space wave function as the migratory electron then couples antiferromagneticly with the Mn ion directly opposite (the three ions involved are collinear). Van Vleck[9] indicates that the migratory electron goes into the $3d$ shell in Mn. Inasmuch as a paramagnetic electron is one which is not paired off with another electron having the same space wave function and opposite spin, the addition of an electron from oxygen reduces (for this excited state) the number of unpaired electrons in the Mn ion from 5 to 4. The expected reduction in magnetic scattering from Mn ions in MnO is discussed in Part VI.

IV. THEORY OF MAGNETIC SCATTERING

Halpern and Johnson[10] give the following expression for the differential cross section $d\sigma/d\omega$ for the magnetic scattering of neutrons from uncoupled paramagnetic

[7] P. W. Anderson, Phys. Rev. **79**, 350, 705 (1950).
[8] J. S. Smart, Phys. Rev. **86**, 968 (1952).
[9] J. H. Van Vleck, Lecture Notes for Grenoble Conference, 1950, unpublished.
[10] O. Halpern and M. H. Johnson, Phys. Rev. **55**, 898 (1939).

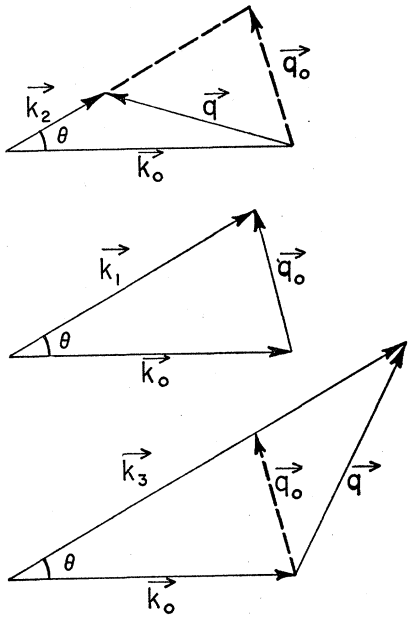

FIG. 4. Vector diagrams of neutron momentum change $\hbar\mathbf{q}$ when scattering is inelastic, elastic, and hyperelastic.

ions:

$$d\sigma/d\omega=\tfrac{2}{3}S(S+1)[e^2\gamma/mc^2]^2F. \quad (1)$$

S is the spin of the ion, e is the charge on the electron, γ is the magnetic moment of the neutron in Bohr magnetons, m is the mass of the electron, and c is the velocity of light. F is the magnetic form factor, and is a function of the neutron momentum change. These authors derive an expression for the differential form factor F, assuming the charge distribution of the $3d$ electrons can be represented by a hydrogenic type wave function.

A theory of neutron scattering from systems of coupled ions which properly considers all the factors involved has not been developed. Halpern and Johnson indicate how the problem should be set up in a general fashion, and comment on the difficulty of evaluating the resulting expressions. Van Vleck[4] estimates the reduction in the paramagnetic scattering due to the inelastic nature of the collisions, and considers the following two processes:

(1) The total differential cross section for vanishingly weak coupling is obtained by employing sum theorems over all final states of the lattice. When the scattering is inelastic, a fraction of these final states will be energetically forbidden, since the energy changes involved are the order of magnitude of the neutron kinetic energy. The forbidden states would require the neutron to loose more than its full kinetic energy. The scattering will be reduced by the loss of these terms, and we refer to this effect as the "inelastic loss of transition states."

(2) For a given scattering angle θ, the value of the neutron momentum change $\hbar\mathbf{q}$ depends on the energy transfer, as indicated in Fig. 4. $\mathbf{k}_0$ is the incident neutron propagation vector. Three cases are illustrated: $|\mathbf{k}_1|=|\mathbf{k}_0|$ corresponds to elastic scattering for which $\mathbf{q}\equiv\mathbf{q}_0$. $|\mathbf{k}_2|<|\mathbf{k}_0|$ corresponds to an inelastic collision, where the neutron looses energy. $|\mathbf{k}_3|>|\mathbf{k}_0|$ corresponds to a hyperelastic collision, where the neutron gains energy. The importance of the diagrams is to note that $\mathbf{q}$ is always larger than $\mathbf{q}_0$ when there is appreciable energy transfer. Since the ionic form factor decreases with increasing $\mathbf{q}$, the observed cross section when the scattering is inelastic (dependent on some average value of $\mathbf{q}$) will be less than the cross section when the scattering is elastic (dependent on $\mathbf{q}_0$). We refer to this as the "inelastic effect on the form factor."

Van Vleck's paper is an important contribution to this subject; we should, however, note the limitations of his calculation. In order to estimate the effect of loss of transition states on the scattering cross section, it is necessary to assume a shape for the distribution curve of frequency of scattering events *versus* energy transfer and to calculate some parameter, such as the root mean square half-width of the distribution, designated W_{rms}. Van Vleck assumes the distribution curve is Gaussian, for which he gives justification. In order to use sum rules when calculating W_{rms}, he assigns equal *a priori* probability to all initial states of the system. This neglects the Boltzmann factor, and, consequently, his calculated value of W_{rms} is for the situation where the temperature T is much larger than the Néel temperature T_0.

It is easy to see that W_{rms} is expected to increase as the temperature is lowered toward T_0. For a simple lattice of ions such as the b.c.t. lattice of MnF_2, if only nearest neighbor interactions are considered, the energy of the spin lattice is given approximately by

$$H=\text{constant}-J\textstyle\sum_i\sum_j \mathbf{S}_i\cdot\mathbf{S}_j, \quad (2)$$

where J is the Heisenberg exchange integral (a negative quantity in an antiferromagnetic compound like MnF_2), and $\mathbf{S}$ is the angular momentum of the Mn ion $(5/2\hbar)$. The sum over i is over all ions in the lattice, and the

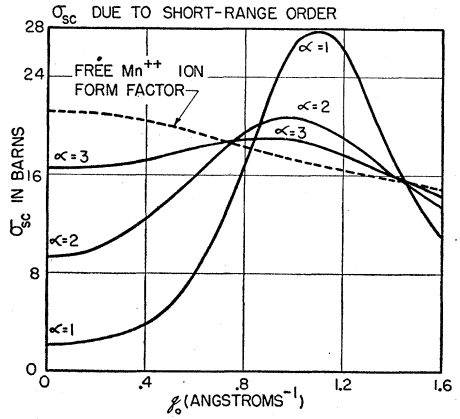

FIG. 5. Scattering cross-section curves obtained by superimposing short-range order scattering on the magnetic form factor.

sum over j is over the nearest neighbors of each ion i. The average value of $|\sum_j \mathbf{S}_j|$ of the neighboring spins of the ith ion is larger at lower temperatures, increasing from the high temperature value of approximately $Z^{\frac{1}{2}}|\mathbf{S}_j|$, where Z is the number of neighbors, to some value approaching $Z|\mathbf{S}_j|$, as T_0 is approached. Hence, the energy required to change the orientation of the ith spin in the field of its neighbors is larger at lower temperatures, and this corresponds to larger energy transfer W in an inelastic scattering event.

Probably the most serious deficiency in Van Vleck's theory is the neglect of residual coherence resulting from short-range order. Consider the equation for coherent scattering, where the scattering amplitude from the lth atom is A_l and we assume a $1/v$ detector:

$$\frac{d\sigma}{d\omega}=\frac{F}{N}\Big|\sum_l A_l e^{-i\mathbf{q}\cdot\mathbf{r}_l}\Big|^2-\frac{F}{N}\sum_l A_l^2,$$
$$\frac{d\sigma}{d\omega}=\frac{F}{N}\sum_l\sum_{l'\neq l} A_l A_{l'} e^{-i\mathbf{q}\cdot(\mathbf{r}_l-\mathbf{r}_{l'})}. \tag{3}$$

F is the form factor for a free ion, N is the number of ions in the crystal, and $\mathbf{r}_l$ is the position vector of the lth ion. For paramagnetic scattering, the essential features are obtained if we let $A_l=\pm A$. If there is correlation between the spins of the l and l' ions, one can write $\bar{A}_{l'}=g(\mathbf{w}_{ll'})A_l$. $\bar{A}_{l'}$ is the average value of $A_{l'}$ when the number of steps along the x, y, and z crystal axes separating the l and l' ions are given by the components of the vector $\mathbf{w}_{ll'}$, and where $g(\mathbf{w}_{ll'})$ is the correlation function.

After replacing $A_{l'}$ with $\bar{A}_{l'}$, we can sum over l in Eq. (3) to obtain

$$\frac{d\sigma}{d\omega}\approx FA^2\sum_{l'\neq l} g(\mathbf{w}_{ll'})e^{-i\mathbf{q}\cdot(\mathbf{r}_l-\mathbf{r}_{l'})}. \tag{4}$$

$\mathbf{r}_l$ is now any representative lattice position, not on the surface of the crystal. The sum over l' is over all ions except the lth ion. Equation (4) gives a liquid-type scattering pattern. In the present experiment, this effect causes a broad peaking of the scattering cross section curve for MnO in the region $|\mathbf{q}_0|\approx 1.23$ reciprocal angstroms and a depletion of the scattering for values of $|\mathbf{q}_0|$ less than 0.9 reciprocal angstroms. The peaking occurs around the location of the sharp magnetic Bragg reflection observed when the sample temperature is below T_0. The Bragg reflection is a result of long-range order, while the liquid-type peak results from local correlation of ion spin directions.

In order to estimate the range of spin order in the samples, we have calculated $d\sigma/d\omega$ from Eq. (4) for MnO, where alternate Mn ions on each sublattice tend to align themselves oppositely. We assumed the following form for the correlation function:

$$g(\mathbf{w}_{ll'})=(-1)^{a+b+c}e^{-\alpha(a+b+c)}. \tag{5}$$

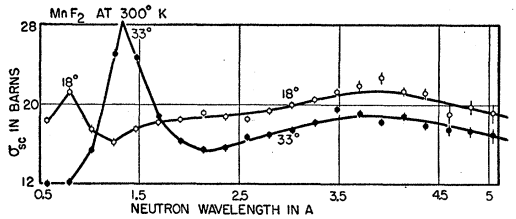

FIG. 6. Neutron scattering by MnF_2 at 300°K.

a, b, and c are the number of steps measured along the x, y, and z crystal axes which separate the two ions being considered. a, b, and c are always positive integers. α is a parameter indicating the range of order; $1/\alpha$ is the distance (in units of the crystal cell dimension 4.435 angstroms) in which the correlation drops to $1/e$. The factor $(-1)^{a+b+c}$ accounts for the alternate spin direction of ions on the sublattice.

The choice of the above function for $g(\mathbf{w}_{ll'})$ is arbitrary, but seems reasonable and allows the necessary integrations to be performed to calculate the cross-section curve. It is believed the shape of the cross-section curve is not sensitive to the exact form of $g(\mathbf{w}_{ll'})$. The curves obtained for three values of α, when the coherence is superimposed on the magnetic form factor, are shown in Fig. 5. For the values of α used in Fig. 5, practically no correlation exists between spin directions of ions separated by more than one step.

Slotnick[11] has treated the problem of coherent paramagnetic scattering, using a high temperature approximation. His results are carried to terms in $1/T^2$, and in a footnote, Slotnick observes that the rapid convergence of terms in inverse powers of T depends on the smallness of the ratio $|\Theta/T|$, where Θ is the temperature constant in the Weiss-Curie Law for the magnetic susceptibility $\chi=C/(T-\Theta)$. For MnO, Θ is -610°K, while our measurements were made at T equal to 300°K and lower. For this reason, our measurements cannot validly be compared with Slotnick's calculations.

Slotnick predicts that the maximum of the coherent scattering peak should be shifted at high temperature from the location of the antiferromagnetic Bragg reflection (determined by the spacing of next nearest neighbors). The shift is derived from nearest neighbor coupling, and the direction of the shift is to larger values of $\mathbf{q}_0$. In this experiment, we observe no shift in the location of the MnO peak. Coherent scattering by MnF_2 was observed only at 126°K, and the peak is too broad to locate the maximum.

V. RESULTS FOR MnF_2

On graphs of the experimental data, we have adopted the convention of plotting $4\pi(d\sigma/d\omega)$ and calling this quantity σ_{sc}. The total scattering cross section would equal σ_{sc} if the scattering were spherically symmetric with the same intensity as is observed in the direction of the counter tubes.

[11] M. Slotnick, Phys. Rev. 83, 1226 (1951).

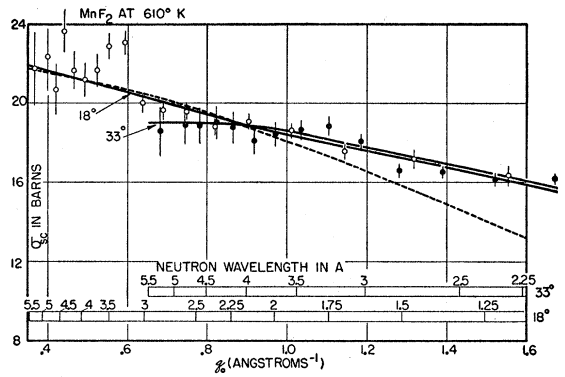

FIG. 7. Neutron scattering by MnF_2 at 610°K. The dashed line is the free ion magnetic scattering cross section calculated using expressions by Halpern and Johnson (reference 10).

Figure 6 shows the scattering data obtained from MnF_2 at 300°K as a function of neutron wavelength, and at the two angles 18° and 33°. These curves are typical of the experimental data. The large peak on the left end of each curve is the last nuclear Debye-Scherrer ring; all the other Debye-Scherrer rings come at shorter neutron wavelengths at these angles. The main contribution to the fairly smooth curves to the right of the peaks is from paramagnetic scattering, with about 1 barn contributed by nuclear incoherent and multiple scattering.

The width of the Debye-Scherrer peaks would be expected to be quite narrow if resolution broadening were absent. The time-of-flight resolution function is roughly triangular with a width at the base of between two and three times the wavelength spacing between adjacent points. In addition, these peaks are further broadened by the angular width of the rings of counter tubes. The angular width is about 4° on either side of the mean scattering angle for half-maximum detection efficiency. Since the paramagnetic scattering is generally a slowly varying function of wavelength, most of the curves are not appreciably distorted by resolution effects.

In order to study the effects of coupling between the Mn ions, the experimental data for MnF_2 at 610°, 300°, and 126°K has been plotted in Figs. 7–9 as a function of q_0, which is $1/\hbar$ times the magnitude of the neutron momentum change for elastic scattering. It may be noted that $q_0=|\mathbf{q}_0|=2|\mathbf{k}_0|\sin(\theta/2)$, where θ is the scattering angle. $\mathbf{k}_0$ is the propagation vector of the incident neutrons, and its magnitude is 2π divided by the wavelength; hence the units of q_0 are reciprocal angstroms. On Figs. 7, 8, and 9 the positions of the experimental points are reversed left for right relative to Fig. 6. Only the part of the curve where paramagnetic scattering can be studied is shown (the nuclear Debye-Scherrer peaks are off the figures to the right). Wavelength scales for each angle are given at the bottom of the figures. For a given angle, neutron energy increases from left to right (the neutron energy E in electron volts is related to the wavelength λ in angstroms by the expression $E=0.0818/\lambda^2$).

On the plots as a function of q_0, the magnetic form factor should be the same for the two angles. The separation between the 18° and 33° curves is caused by inelastic scattering, which is different at the two angles, inasmuch as neutrons at 33° have only 0.3 the energy of neutrons at 18° for the same q_0.

The differential cross section for magnetic scattering calculated from Eq. (1), using an expression for the magnetic form factor F derived by Halpern and Johnson,[10] is shown on Fig. 7 as a dashed line.[12] In calculating F, the mean radius for the $3d$ electron probability function was taken to be 0.64 angstroms, the value determined by Ruderman.[1] Except for three points at small values of q_0, which are probably raised due to nuclear coherent scattering into the plane of the sample (see Part II), the experimental data at 18° agrees well with the dashed line in the region $q_0<0.9$. The 18° curve is essentially unaffected by coupling between ions, which is very small at this temperature (610°K). Thus the 18° curve in Fig. 7 is considered to be an experimental determination of the magnetic scattering from free ions. The agreement of experimental points with the dashed line for values of $q_0<0.9$ confirms the derivation by Halpern and Johnson of Eq. (1).

It is seen that the experimental curves lie above the dashed line for $q_0>0.9$. This indicates the radial distribution of the $3d$ electrons in Mn ions decreases faster at large radii than the free ion wave functions used by Halpern and Johnson. Shull[2] has mentioned that this compression of the wave functions may be the result of neighboring ions in the crystal lattice.

In Figs. 7–9 it is seen that the 33° curve drops below the 18° curve for $q_0<0.9$. This separation is attributed to the two inelastic processes described by Van Vleck (see Part IV). It is of interest to evaluate the half-width W_{rms}, the parameter indicating the amount of energy exchanged in inelastic collisions, using Van Vleck's assumption of a Gaussian distribution of frequency of scattering events *versus* energy transfer. This is done by assuming the fraction of the cross section at 18° which is included in the separation between the curves

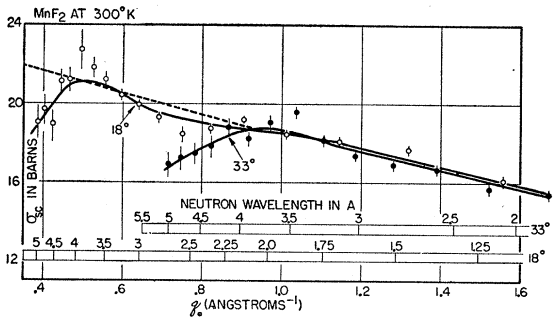

FIG. 8. Neutron scattering by MnF_2 at 300°K.

[12] The dashed line has been raised by one barn for comparison with experimental points.

equals the loss of scattering due to inelastic processes at the lower energy (33° curve). The energies for points at corresponding values of q_0 on the 18° curve are so high that they have essentially no loss of scattering. We then assume some part of this separation (for example, $\frac{3}{4}$ of the separation) is derived from the loss of transition states. This loss is that portion of a Gaussian distribution which extends to one side of the mid-point a distance greater than the incident neutron energy. From the loss of states and the incident neutron energy, the half-width of the distribution is found using tables of the Standard Error Function. The loss produced by the inelastic effect on the form factor is then calculated, making use of this tentative value of W_{rms}. If the sum of these effects does not give the observed separation between the curves, the calculation is repeated assuming a slightly different value for the loss of transition states.

For the 610°K data, the four lowest energy points (smallest values of q_0) on the 33° curve give W_{rms} equal to 0.00196, 0.00195, 0.00203, and 0.00196 ev.[13] These are in good agreement with each other and give an average for W_{rms} equal to about 0.0020 ev. On the average, the loss of transition states accounts for 80 percent of the separation between curves.

On Fig. 8, at 300°K, the four lowest energy points on the 33° curve correspond to W_{rms} equal to 0.00267, 0.00264, 0.00265, and 0.00261 ev. These values also show internal agreement and average about 0.0026 ev, which is markedly larger than the value for 610°K. The loss of transition states accounts for 73 percent of the separation between curves.

For 126°K, inspection of Fig. 9 shows that the low energy points at 33° do not form a smooth curve (the irregularity may be accounted for by statistical fluctuations). The values indicated by the seven lowest energy points are 0.00335, 0.00357, 0.00405, 0.00401, 0.00288, 0.00277, and 0.00303 ev. An average value for W_{rms} of about 0.0034 ev is indicated. The loss of transition states accounts for 74 percent of the separation between curves. The experiment confirms that W_{rms} increases as the temperature is lowered, as discussed in Part IV. The experimental values agree in order of magnitude with the value of W_{rms} calculated using Van Vleck's formulas,[4] which give, for $T \gg T_0$, $W_{\text{rms}}=0.00285$ ev.

Mention should be made of how the above results compare with those found by Shull, Strausser, and Wollan.[2] They found no change in scattering data when they raised the temperature of their MnF_2 sample from room temperature to 400°C. This can be explained by the comparatively high energy of their neutrons, which had a wavelength of 1.057 angstroms. At wavelengths shorter than 2 angstroms, we observe no change between 300° and 610°K. Our measurements are sensitive to inelastic effects only because they are extended to include very low energy neutrons. Shull and his coworkers also mention that their MnF_2 curve falls 10 percent below the basic cross section in the forward direction of $21.2/4\pi$ barns/steradian calculated by Halpern and Johnson using Eq. (1). While there is an uncertainty of about one barn in our measurements, we appear to observe (in Fig. 7) the full value of 21.2 barns.

[13] The experimental values of W_{rms} were computed using the experimental points for 33° and the smooth curve drawn for 18°.

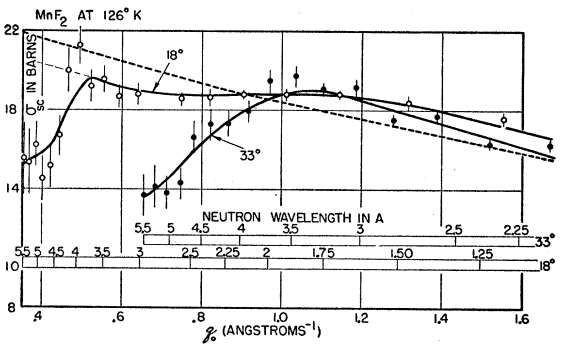

FIG. 9. Neutron scattering by MnF_2 at 126°K.

The magnetic scattering curve obtained at a scattering angle of 18° and temperature of 610°K has been drawn on Figs. 8 through 11 as a dashed line for reference purposes. An additional effect connected with the loss of scattering produced by inelastic processes may be noted on Figs. 8 and 9. By referring to the wavelength scales on these figures, points having the same wavelength, and hence the same neutron energy, may be identified on the curves at the two angles. We note the fractional separation between the curves at a particular wavelength for the 33° curve, and we add this as a correction to the 18° curve on the same figure, at the corresponding wavelength for 18°. This correction is made between 4 and 5.5 angstroms. The result of applying this correction to the data for 300°K is to bring the 18° curve up to the dashed line representing the free ion magnetic scattering curve. Apparently, inelastic scattering reduces the neutron scattering at the two angles by the same amount at corresponding neutron energies.

The consequence of applying the above correction to Fig. 9, showing data taken at 126°K, is to raise the 18° points to give a smooth curve, lying perhaps 1.5 barns below the free ion magnetic scattering curve, in the region $q_0<0.6$. The 18° curve, which rises above the free ion curve for $q_0>1.0$, then resembles the curves shown in Fig. 5. The curves in Fig. 5 were calculated to illustrate the effect of residual coherent scattering resulting from correlation of the spin directions of neighboring ions in the crystal lattice. The correction we have made is for inelastic scattering and allows the short-range order scattering to appear. An estimated value for the short-range order parameter α for MnF_2 at 126°K is about 4. Short-range order scattering is not detected in the curves at higher temperatures.

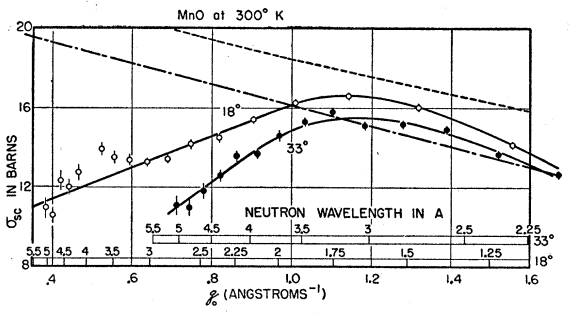

FIG. 10. Neutron scattering by MnO at 300°K.

The results obtained for MnF_2 are summarized as follows:

(1) At a scattering angle of 18° and a temperature of 610°K, the neutron scattering is essentially from uncoupled Mn ions, and the differential cross section for magnetic scattering from free ions is observed. The cross section at small values of q_0 confirms the derivation of the paramagnetic scattering by Halpern and Johnson. The shape and height of the curve for large values of q_0 show the *3d* electron distribution in Mn^{++} decreases faster for large radii than the hydrogenic wave functions used by Halpern and Johnson.

(2) The separation between the curves at 18° and 33° plotted as a function of q_0 is attributed to inelastic scattering processes at the 33° angle, where the neutron energy is lower. Assuming a Gaussian distribution for energy transfer to the spin lattice, W_{rms} increases with decrease in sample temperature as follows:

Temperature:	610°K	300°K	126°K
W_{rms}:	0.0020 ev	0.0026 ev	0.0034 ev

(3) At 300°K and 126°K, inelastic scattering appears to reduce the scattering at the two angles by the same amount at corresponding neutron energies.

(4) Residual coherent scattering due to short-range order is not observed at 610° or at 300°K, but affects the scattering to the extent of 1.5 barns at 126°K.

VI. RESULTS FOR MnO

The cross section data at the temperatures 300° and 133°K are plotted as a function of q_0 in Figs. 10 and 11. The shape of the 18° curve at 300°K indicates it has been distorted by short-range order scattering. Shull, Strauser, and Wollan[2] also observe short-range order scattering by MnO at room temperature. As nearly as we can tell from their Fig. 1, the location and maximum of their peak are the same as we observe. The maximum cross section, when multiplied by 4π steradians, is about 15.6 barns. At the location of the maximum, their value of the cross section for MnF_2 (determined by the free ion magnetic scattering) is about 13.6 barns, while we observe 16.6 barns (the MnF_2 magnetic scattering curve is drawn as a line of short dashes in Figs. 10 and 11).[14] Therefore, while the MnO peak rises above their free ion magnetic scattering curve (as it should, due to short-range order scattering) by about 2 barns, it lies below our free ion magnetic scattering curve by about 1 barn.

We believe our curve for magnetic scattering from free ions is correct and propose an explanation for our results. The explanation is that the cross section for magnetic scattering [Eq. (1)] may be lower for MnO, as a result of the mechanism of super-exchange. As discussed in Part III, the total wave function of the Mn ion in MnO is believed to include excited states in which the number of paramagnetic electrons is reduced from 5 to 4. Referring to Eq. (1), the magnetic scattering cross section depends on $S(S+1)$, where S is the (spin) angular momentum of the Mn ion in units of $\hbar$, and therefore depends on the number of paramagnetic electrons in the ion. The situation is very complex; but, taking the simplest possible view, we conclude that if the excited state involved in super-exchange was occupied all of the time, the smaller value of $S(S+1)$ could reduce the magnetic scattering from Mn to 24/35 of its free ion value. From the shape of the 18° curve in Fig. 10, we roughly estimate that in the region of the peak, the magnetic scattering curve should lie about 1.5 barns below the peak of this curve, and thus about 2.5 barns below the magnetic scattering curve for MnF_2. A line of long dashes representing this estimate has been drawn on the figures. This reduction in magnetic scattering corresponds to occupation of the excited state about 45 percent of the time.

One would like to evaluate W_{rms} for MnO by an analysis of the separation between the 18° and 33° curves, as was done for MnF_2. This cannot be done reliably because the MnO curves are displaced by large short-range order scattering, in addition to the inelastic effects with which we would identify the separation.

The experimental curves in Figs. 10 and 11 show the peaking in the region $q_0 \approx 1.2$ increases as the temperature is lowered. The value of the cross section for $q_0 < 1.0$ is lower at the lower temperature. The depletion of the 18° curve at small values of q_0 may be a result both of larger short-range order scattering effects and of greater inelastic effects at the lower temperature.

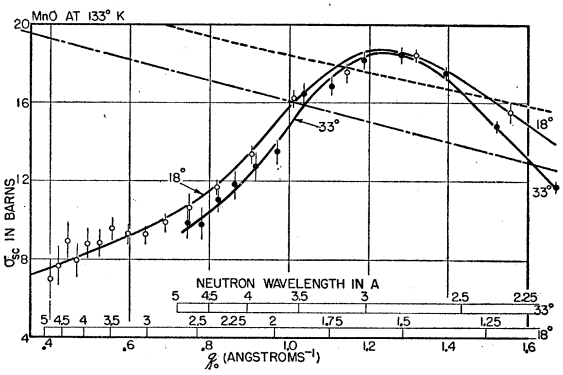

FIG. 11. Neutron scattering by MnO at 133°K.

[14] The dashed lines are raised one barn to account for nuclear incoherent and multiple scattering.

The range of spin order at 300°K and 133°K was estimated by comparing the shape of the experimental curves at 18° with the shape of the calculated curves shown in Fig. 5. In order to make the comparison, it was estimated very roughly that inelastic effects account for one-half the separation between the experimental curves and the line drawn with long dashes, in the region $q_0<1.0$. From the shape of the experimental curves, we estimate rough values of α to be 3 and 2, at 300° and 133°K, respectively. The amount of order is seen to increase with decreasing temperature. However, these values of α are sufficiently large to indicate that most of the correlation of spin direction exists only between adjacent ions on the same sublattice. As long-range ordering is expected below the Néel temperature, a large change in ordering apparently takes place close to the Néel temperature.

Figure 12 shows data taken at 107°K, 15° below the Néel temperature, plotted as a function of neutron wavelength λ. The peaks furthest to the left, occurring at λ equals 0.8 and 1.4 angstroms for 18° and 33°, respectively, result from nuclear Debye-Scherrer reflection from (1,1,1) planes. The two larger peaks, occurring at λ equals 1.6 and 2.8 angstroms for 18° and 33°, respectively, are produced by the magnetic Debye-Scherrer reflection from (1,1,1) planes on a double-spaced lattice. These peaks, previously observed by Shull and Smart,[15] result from long-range antiferromagnetic order of the crystal spins. They occur at $q_0=1.23$. The nuclear and magnetic peaks on the 18° curve are not fully resolved.

Owing to the long-range spin order below T_0, coherent effects predominate in Fig. 12. The magnetic form factor has disappeared, and the magnetic scattering is concentrated almost entirely in crystal reflections. For the 33° curve, we have compared the area under the magnetic peak with the area under the nuclear peak, and we find that the total "scattering power" of the magnetic Debye-Scherrer ring is consistant with long-range order and a unit cell of sides 8.870 angstroms. It is not possible to tell if the four sublattices are scattering coherently or independently, for theoretically the area under the Debye-Scherrer ring is the same in either case.

[15] C. G. Shull and J. S. Smart, Phys. Rev. **76**, 1256 (1949).

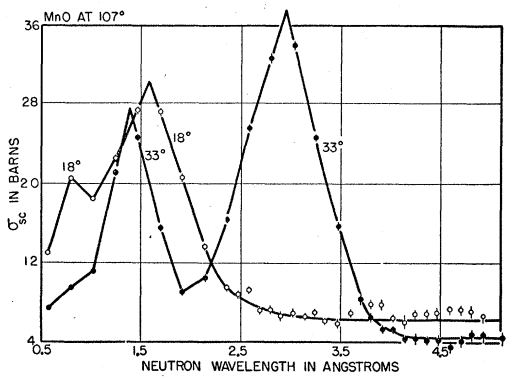

FIG. 12. Neutron scattering by MnO at 107°K.

The results for MnO are summarized as follows:

(1) The curves at 300°K indicate the magnetic scattering cross section for MnO, if it were not distorted by short-range order scattering, would be about 2.5 barns smaller than for MnF_2. We suggest this can be accounted for by the mechanism of super-exchange.

(2) Comparison of the shape of the experimental curves with calculated curves indicates values of the short-range order parameter α to be 3 and 2, at temperatures of 300° and 133°K, respectively. The amount of spin order is found to increase with decrease in temperature, but most of the correlation of spin direction exists only between adjacent ions on the same sublattice. This indicates a large change in ordering takes place near the Néel temperature.

(3) The (1,1,1) magnetic Debye-Scherrer reflection from a double-spaced lattice is observed at 107°K. This confirms long-range antiferromagnetic ordering exists below T_0.

The author wishes to express his appreciation to Professors L. James Rainwater and W. W. Havens, Jr., for real assistance they rendered to all phases of the research. He is also grateful to Dr. I. W. Ruderman for preparing the samples, and to Dr. Murray Slotnick for helpful discussions on the interpretation of results. The assistance of Janet E. Bendt, and of persons working on the cyclotron staff, is gratefully acknowledged.

The author thanks the U. S. Atomic Energy Commission for its support of this research. He is also indebted to the Vanadium Corporation of America for the loan of a pure vanadium sample.